- Frictional boundary layer in a low Ro rotating fluid (at solid surface or air/water interface).

$$\frac{D\vec{u}_h}{Dt} + f\hat{k}\times\vec{u}_h = -\frac{1}{\rho}\nabla_h p + \nu\nabla^2\vec{u}_h$$

For laminar flow in the interior of the fluid, with $Ro \ll 1$ and $H \lesssim L$,

$$\frac{[\nu\nabla^2\vec{u}_h]}{[LHS]} \approx \frac{[\nu\nabla^2\vec{u}_h]}{[f\vec{k}\times\vec{u}_h]} = \frac{\nu U/H^2}{fU} = \frac{\nu}{fH^2} = Ek.$$

For air, $\nu \approx 1.4\times10^{-5}\,\frac{m^2}{s}$. If $H = 10\,km$, $Ek \approx 10^{-9}$
For ocean, $\nu \approx 10^{-6}\,\frac{m^2}{s}$. If $H = 1\,km$, $Ek \approx 10^{-8}$
} Thus molecular viscosity in unimportant in interior of fluid, except where there is turbulence.

However, friction must become important where fluid adjusts to a bdry. For a rigid horizontal bdry, $\vec{u}(bdry) = 0$. There is a thin "boundary layer" in which this adjustment takes place in which

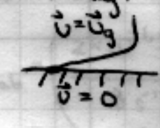

$$1 \sim \frac{[\nu\nabla^2\vec{u}_h]}{[f\vec{k}\times\vec{u}_h]} \sim \frac{\nu U/d^2}{fU} \Rightarrow \quad d = \left(\frac{2\nu}{f}\right)^{\frac{1}{2}}, \quad Ek = (d/H)^2$$

For air, laminar Ekman layer depth is 0.5 m with $f = 10^{-4}\,s^{-1}$
For H_2O, " " " " " " is 0.15 m " " "
and 0.5 mm with $f = 8\,s^{-1}$ ($\Omega = 33$ rpm).

Observed wind-driven BL's are O(200-1000 m) deep in atm, O(5-30 m) deep in ocean
$\Rightarrow$ larger turbulent "eddy viscosity" $\nu_{air} = \frac{f}{2} d_{air}^2 = 2\text{-}50\,\frac{m^2}{s}$, $\nu_{ocean} = \frac{f}{2} d_{oc}^2 = 0.001\text{-}0.05\,\frac{m^2}{s}$.

Bottom Ekman layer in steady homogeneous flow (Gill 9.6 has a terse discussion)

Idealizations: steady $\left(\frac{\partial}{\partial t} = 0\right)$, horizontal homogeneous $\left(\frac{\partial}{\partial x} = \frac{\partial}{\partial y} = 0\right)$, f-plane, constant density ρ, spatial uniform horizontal pressure gradient force $\propto -\frac{\nabla_h p}{\rho}$.

Look for soln $(u(z), v(z))$ with:

$u(0) = v(0) = 0$ (No slip at bottom boundary $z = 0$)

$-fv = -\frac{1}{\rho}\frac{\partial p}{\partial x} \equiv -fv_g$ and $fu = -\frac{1}{\rho}\frac{\partial p}{\partial y} \equiv fu_g$ as $z \to \infty$ (No frictional effects far from boundary)

Note that since $w(0) = 0$ and $\frac{\partial u}{\partial x} + \frac{\partial v}{\partial y} = 0$, $w(z) = w(0) - \int_0^z \left(\frac{\partial u}{\partial x} + \frac{\partial v}{\partial y}\right)dz = 0$.

Thus
$$\frac{Du}{Dt} = \underbrace{\frac{\partial u}{\partial t}}_{0} + \underbrace{u\frac{\partial u}{\partial x}}_{0} + \underbrace{v\frac{\partial u}{\partial y}}_{0} + \underbrace{w\frac{\partial u}{\partial z}}_{0} = 0 \quad \text{+ similarly for } v.$$

and $\nabla^2 u = d^2u/dz^2$ + similarly for v. Thus, hor. mom. eqns become:

$$\frac{Du}{Dt} - fv = -\frac{1}{\rho}\frac{\partial p}{\partial x} + \nu\nabla^2 u \longrightarrow -f(v - v_g) = \nu\frac{d^2u}{dz^2} \qquad (1)$$

$$\frac{Dv}{Dt} + fu = -\frac{1}{\rho}\frac{\partial p}{\partial y} + \nu\nabla^2 v \longrightarrow f(u - u_g) = \nu\frac{d^2v}{dz^2} \qquad (2)$$

35

Setting $s = u + iv$ and $s_g = u_g + iv_g$, we find (1) + i(2) ⇒

$$\nu \frac{d^2 s}{dz^2} = -f(v - v_g) + if(u - u_g) = if(s - s_g)$$

The homogeneous eqn has characteristic polynomial $\nu r^2 - if = 0 \Rightarrow r_{1,2} = \pm e^{\frac{i\pi}{4}}\left(\frac{f}{\nu}\right)^{\frac{1}{2}}$

The positive root r_1 has positive real part so $e^{r_1 z} \to \infty$ as $z \to \infty$, inconsistent with BC. In addition, $s = s_g$ is an inhomogeneous soln by inspection, so

$$s(z) = s_g + c_2 e^{r_2 z}$$

Noting that $r_2 z = -\frac{(1+i)}{\ } \left(\frac{f}{2\nu}\right)^{\frac{1}{2}} z = -(1+i)\zeta$, $\zeta \equiv \frac{z}{d}$, d = Ekman depth,

and applying BC $s(0) = 0$, we see $c_2 = -s_g$ and

$$s(z) = s_g\left\{1 - e^{-(1+i)\zeta}\right\}.$$

Setting $s_g = u_g$ (positive real) corresponding to eastward geostrophic wind, we see

$$u + iv = u_g\left\{1 - e^{-\zeta}(\cos\zeta - i\sin\zeta)\right\} \Rightarrow \boxed{u(z) = u_g(1 - e^{-\zeta}\cos\zeta),\ v(z) = e^{-\zeta}\sin\zeta}$$

(1) Near $z = 0$, $u(z)$ and $v(z)$ both $\approx \zeta$ so surface wind is 45° to left of geostrophic, ...

(2) and surface wind stress of air on surface (equal and opposite to drag of surface on air):

$$\vec{\tau} = \rho\nu\, d\vec{u}/dz(0) = \frac{\rho\nu}{d}(\hat{\imath} + \hat{\jmath})$$

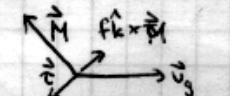

(3) Net frictional transport

$$\vec{M}_E = \int_0^\infty \rho(\vec{u} - \vec{u}_g)\,dz = \rho u_g d\left[-\hat{\imath}\underbrace{\int_0^\infty e^{-\zeta}\cos\zeta\,d\zeta}_{\frac{1}{2}} + \hat{\jmath}\underbrace{\int_0^\infty e^{-\zeta}\sin\zeta\,d\zeta}_{\frac{1}{2}}\right]$$

Note $f\hat{k}\times\vec{M} = \vec{\tau}$.

For a general flow direction $\vec{u}_g$:

$$\vec{M} = \rho d\left\{u_g\left[-\frac{\hat{\imath}}{2} + \frac{\hat{\jmath}}{2}\right] + v_g\left[-\frac{\hat{\jmath}}{2} - \frac{\hat{\imath}}{2}\right]\right\}$$

$$\boxed{\vec{M}_E = \frac{\rho d}{2}\left\{-(u_g + v_g)\hat{\imath} + (u_g - v_g)\hat{\jmath}\right\}.}$$

Nonuniform currents + Ekman pumping

Now suppose $u \approx u_g(x,y)$ and $v \approx v_g(x,y)$. For a truly homogeneous fluid this is the only low Ro horizontal inhomogeneity that can be supported. Suppose u_g, v_g vary on a lengthscale $L \gg \delta$. Then locally frictional BL eqns look as before with u_g, v_g = local values. Note that the frictional flow is divergent even though (u_g, v_g) is not:

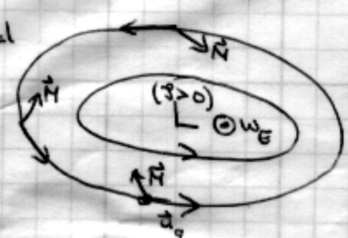

$$D = \frac{\partial M_x}{\partial x} + \frac{\partial M_y}{\partial y} = \frac{\rho d}{2}\left\{-\frac{\partial}{\partial x}(u_g + v_g) + \frac{\partial}{\partial y}(u_g - v_g)\right\}$$
$$= -\frac{\rho d \zeta_g}{2}$$

This must result in a vertical velocity

$$w_E = \lim_{z\to\infty}\int_0^z \frac{\partial w}{\partial z}\,dz = \int_0^z -\left(\frac{\partial u}{\partial x} + \frac{\partial v}{\partial y}\right)dz = -D/\rho = \frac{d}{2}\zeta_g \quad \text{"Ekman pumping"}$$

Effect on interior $\frac{1}{f}\left(\frac{d\zeta}{dt}\right)_E = \frac{1}{h}\underbrace{\left(\frac{dh}{dt}\right)_E}_{-w_E}$

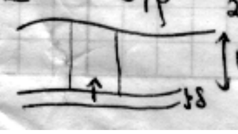

The Ekman Layer (figures from Cushman-Roisin)

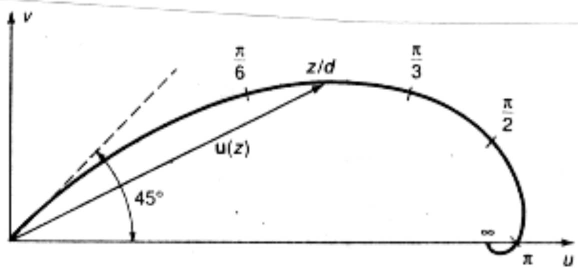

Figure 5-2 The velocity spiral in the bottom Ekman layer. The figure is drawn for the Northern Hemisphere ($f > 0$), and the deflection is to the left of the current above the layer. The reverse holds for the Southern Hemisphere.

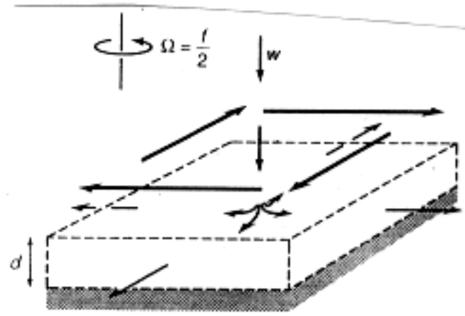

Figure 5-3 Divergence in the bottom Ekman layer and compensating downwelling in the interior. Such situation arises in the presence of an anticyclonic gyre in the interior. Similarly, interior cyclonic motion causes convergence in the bottom Ekman layer and upwelling in the interior.

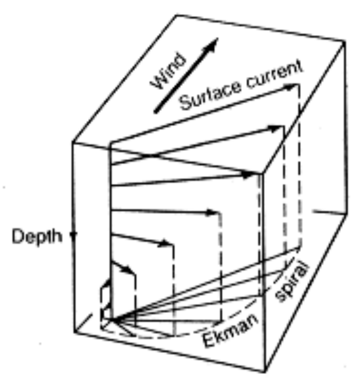

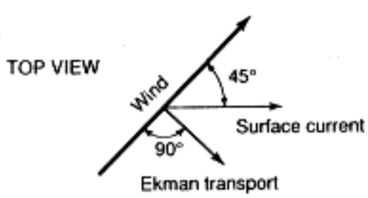

Figure 5-5 Structure of the surface Ekman layer. The figure is drawn for the Northern Hemisphere ($f > 0$), and the deflection is to the right of the surface stress. The reverse holds for the Southern Hemisphere.

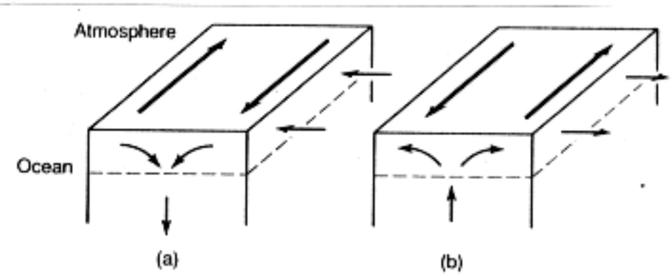

Figure 5-6 Ekman pumping in an ocean subject to sheared winds (Northern Hemisphere).

GFD

Real Geophysical Ekman Layers

Atmosphere

Turbulence

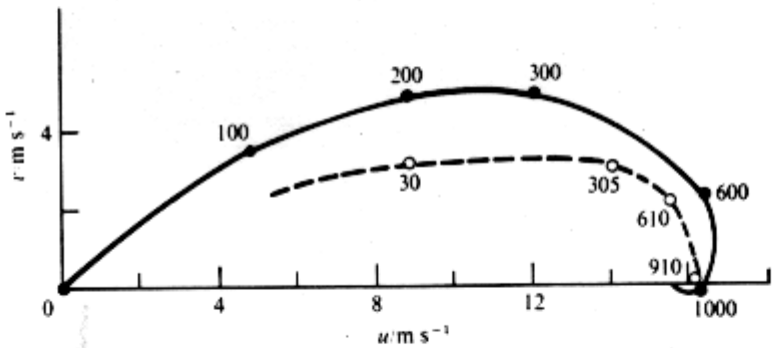

Fig. 9.2. Wind hodograph for the lowest kilometre as measured by Dobson (1914) (dashed line) compared with Ekman spiral (full line). Figures on curves are heights in metres.

Ocean

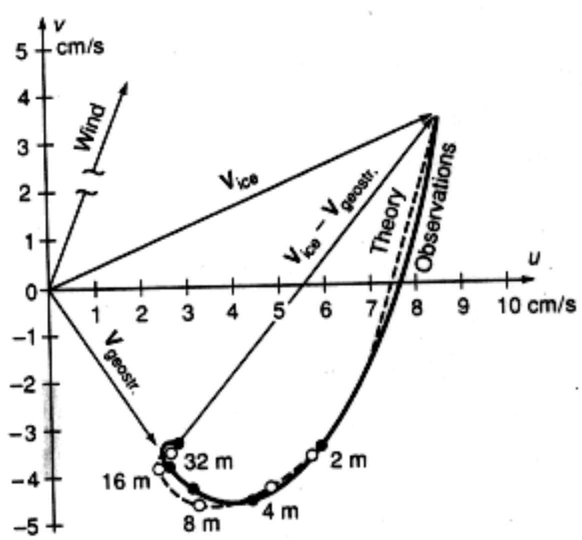

Figure 5-7 Comparison between observed currents below a drifting ice floe at 84.3°N and theoretical predictions based on an eddy viscosity $\nu = 2.4 \times 10^{-3}$ m^2/s. (Reprinted from *Deep-Sea Research*, 13, Kenneth Hunkins, Ekman drift currents in the Arctic Ocean, p. 614, copyright 1966, with kind permission from Pergamon Press Ltd, Headington Hill Hall, Oxford 0X3 0BW, UK.)